

SCIENTIFIC REPORTS



OPEN

Antiretroviral Treatment with Efavirenz Disrupts the Blood-Brain Barrier Integrity and Increases Stroke Severity

Received: 21 August 2016
Accepted: 28 November 2016
Published: 23 December 2016

Luc Bertrand, Levi Dygert & Michal Toborek

The introduction of antiretroviral drugs (ARVd) changed the prognosis of HIV infection from a deadly disease to a chronic disease. However, even with undetectable viral loads, patients still develop a wide range of pathologies, including cerebrovascular complications and stroke. It is hypothesized that toxic side effects of ARVd may contribute to these effects. To address this notion, we evaluated the impact of several non-nucleoside reverse transcriptase inhibitors (NNRTI; Efavirenz, Etravirine, Rilpivirine and Nevirapine) on the integrity of the blood-brain barrier, and their impact on severity of stroke. Among studied drugs, Efavirenz, but not other NNRTIs, altered claudin-5 expression, increased endothelial permeability, and disrupted the blood-brain barrier integrity. Importantly, Efavirenz exposure increased the severity of stroke in a model of middle cerebral artery occlusion in mice. Taken together, these results indicate that selected ARVd can exacerbate HIV-associated cerebrovascular pathology. Therefore, careful consideration should be taken when choosing an anti-retroviral therapy regimen.

The introduction of anti-retroviral drugs (ARVd) changed the prognostic of HIV infection from a terminal to a chronic disease. Patients can lead normal lives and control the infection by adhering to highly active antiretroviral therapy (HAART)^{1,2}. Nevertheless, these patients will likely be under treatment for the rest of their lives, meaning that they will be continually exposed to ARVd. Given the length of exposure, infected patients are at higher risk of developing co-morbidities, such as cardiovascular, metabolic and neurological disease³⁻⁷. While some of these disorders can be attributed to HIV infection and the ensuing persistent state of inflammation, growing evidence indicates that ARVd toxicity could be at least partially involved in the development of these pathologies. Several side effects, such as lactic acidosis, lipodystrophy, hyperbilirubinemia, diarrhea, pancreatitis, peripheral neuropathy, neuropsychiatric disorders and hypersensitivity, have been linked to the use of ARVd⁸⁻¹⁸. HIV protease inhibitors have been associated with proteasome disruption, liver injury, and gut barrier dysfunction¹⁹. Non-nucleoside reverse transcriptase inhibitors (NNRTIs) may be responsible for induction of inflammation²⁰, neurotoxicity, and rashes²¹. While the direct cause of these adverse reactions can be multifactorial, certain NNRTIs, especially Efavirenz, can play an important role given the indications that they can disrupt nitric oxide production, mitochondrial function, ER stress and autophagy²²⁻²⁵.

The long term survival of HIV infected patients makes them more susceptible to the development of cardiovascular diseases²⁶. Several epidemiologic studies denoted that these individuals are younger and present a higher incidence of vasculopathies, cardio- and cerebrovascular diseases than non-infected patients²⁷⁻³⁰. HIV-positive patients who develop stroke often present a different profile than the general population, exhibiting less predisposing symptoms, such as hypertension³¹. Multiple factors linked to the HIV infection can contribute to this increased susceptibility, including chronic vascular inflammation, opportunistic infections, endocarditis, cachexia, coagulation abnormalities, and dyslipidemia. Furthermore, HIV and its proteins can interact directly with the endothelium and contribute to increased incidence of atherosclerosis, a major contributing factor of cardiovascular disease^{32,33}, which can further be exacerbated by antiretroviral treatment. Epidemiological studies demonstrated that while endothelial dysfunction is reduced following HAART initiation, long term exposure to ARVd leads to the development of vasculopathy, especially with the usage of certain protease inhibitors^{34,35}. These

University of Miami Miller School of Medicine, Department of Biochemistry and Molecular Biology, Miami, FL, USA. Correspondence and requests for materials should be addressed to L.B. (email: l.bertrand@med.miami.edu) or M.T. (email: mtoborek@med.miami.edu)

conditions could arise from chronic induction of ER stress^{36,37}, an increase in local inflammation³⁸, or apoptosis activation³⁹.

The blood-brain barrier (BBB) plays a central role in maintaining the homeostasis of the central nervous system (CNS). The BBB protects the brain from toxins, pathogens, and other potential harmful components that can be present in the blood^{40–43}. The BBB is composed of the neurovascular units in which neurons interact with three major cell types: endothelial cells, pericytes, and astrocytes. The brain microvascular endothelial cells (BMEC) are linked together by an assembly of tight junction (TJ) proteins that restrict the passage of molecules at the paracellular space. The main component of these structures are claudins (primarily claudin-5), which are transmembrane proteins that connect the neighboring endothelial cells. These proteins are linked to the cytoskeleton by adaptor proteins, such as zona occludens-1, 2, 3 and cingulin. In addition, several other molecules also play a role in TJ assembly, such as occludin, junctional adhesion molecules, and adherens junction proteins^{40,44}. The regulation of TJs is influenced by the signaling factors originating from BMEC, but also influenced by pericytes and astrocytes^{40,45,46}. Dysfunction of the BBB and the associated increase in BBB permeability is linked to the pathology of several acute and chronic CNS diseases. An uncontrolled trafficking of immune cells to the CNS can lead to inflammation, neuronal loss, and the entry of pathogens, resulting in infections. The loss of control on the flow of molecules in or out of the CNS can contribute to the development of Alzheimer's disease, epilepsy, or stroke⁴⁷. In the context of the present study, it is important that disrupted BBB can increase the extent of tissue damage and mortality in stroke^{48–50}.

Several publications reported that ER stress induction is linked to endothelial dysfunction and can lead to an increased vascular permeability in various disease models^{51–56}. We previously demonstrated that exposure of brain endothelial cells to Efavirenz induces ER stress and disrupts autophagy²⁵. The present study aims to identify the impact of NNRTI-induced toxicity on endothelial functions, such as disruption the barrier integrity and the severity of stroke. Our results demonstrate that of the several NNRTIs tested, only Efavirenz affected endothelial integrity via reduction in claudin-5 expression, and alterations in its phosphorylation. In addition, treatment with Efavirenz resulted in an increase in BBB permeability and enhanced tissue injury in stroke.

Results

Exposure to Efavirenz, but not to other NNRTIs, leads to an increase in endothelial permeability. To evaluate the impact of NNRTI on endothelial permeability, human cerebral microvascular cells (hCMEC) were grown to confluence on Transwell inserts. After the formation of monolayers, the cells were exposed to the indicated conditions for 48 h. Then, media in the apical compartment of the Transwell system was replaced with medium containing fluorescently-tagged dextran. After 90 min incubation, fluorescence intensity in the basal compartment was read using a plate reader. Among studied NNRTIs, exposure to Efavirenz resulted in a significant increase in permeability of hCMEC monolayers for all molecular sizes of dextran tested (Fig. 1A–C). Exposure to the other NNRTIs did not affect the transfer of fluorescent markers across the endothelial monolayer. These results were largely confirmed in cultures of human primary brain endothelial cells (Fig. 1D). However, exposure to Nevirapine slightly increased permeability across the monolayers of primary brain endothelial cells. Such results appear to be consistent with different susceptibility of primary cells compared to a cell line.

Efavirenz, but not other NNRTIs, induces a specific reduction in claudin-5 levels. We next sought to identify the impact of NNRTI exposure on TJ protein levels, given their primordial role in maintaining endothelial barrier function. Cells were exposed to NNRTIs as in Fig. 1 and lysed using RIPA buffer. The expression levels of claudin-5, occludin, and ZO-1, three major TJ proteins, were analyzed by western blotting. A specific reduction in claudin-5 levels was observed in cells exposed to Efavirenz, but not to other NNRTIs (Fig. 2A). On the other hand, occludin and ZO-1 levels remained unaffected, independent of treatment (Fig. 2B and C, respectively). In order to evaluate dose response effects of Efavirenz, we exposed hCMEC to doses ranging from 1 μ M to 10 μ M. Efavirenz at 10 μ M consistently lowered claudin-5 levels; however, treatment with 1 μ M resulted in a significant increase in expression of this protein (Fig. 2D). No significant impact of Efavirenz on endothelial permeability was observed at doses lower than 10 μ M (Fig. 2E).

We also investigated time-dependent effects of Efavirenz exposure on claudin-5 expression and endothelial barrier function. A significant decrease in claudin-5 and endothelial barrier function was confirmed at 48 h of exposure (Fig. 2F and G, respectively). A 12 h treatment with Efavirenz increased claudin-5 levels (Fig. 2F) with no impact on permeability (Fig. 2G). No changes in these parameters were observed in cells exposed to Efavirenz for 24 h.

In human primary brain endothelial cells, exposure to Efavirenz, but not other NNRTIs, lead to a decrease in claudin-5 expression (Fig. 2H). Furthermore, all listed treatments did not impact either occludin or ZO-1 (data not shown), fully confirming the results from a cell line.

Overall, these results indicate that Efavirenz exposure results in an increase in monolayer permeability that correlates with a specific reduction in claudin-5 level. In addition, this effect is contingent on dose and exposure time.

Disruption of intracellular localization of claudin-5 by Efavirenz. In addition to the expression level, cellular localization of TJ proteins is essential for their function. Therefore, we assessed the impact of NNRTIs on claudin-5, occludin, and ZO-1 immunoreactivity. hCMEC were grown to confluence on round coverslips coated with collagen, and exposed to vehicle or NNRTIs for 48 h. Afterward, cells were processed for immunofluorescence to assess cellular localization of TJ proteins. The nuclei were stained with DRAQ5. Using confocal microscopy, we detected a regular colocalization of claudin-5 with ZO-1, and claudin-5 with occludin in cells treated with DMSO, Etravirine, Nevirapine and Rilpivirine (Fig. 3A and B). In contrast, in cells exposed to Efavirenz, this co-localization was absent due to both a severe reduction in the presence of claudin-5 from cell-cell junctions and

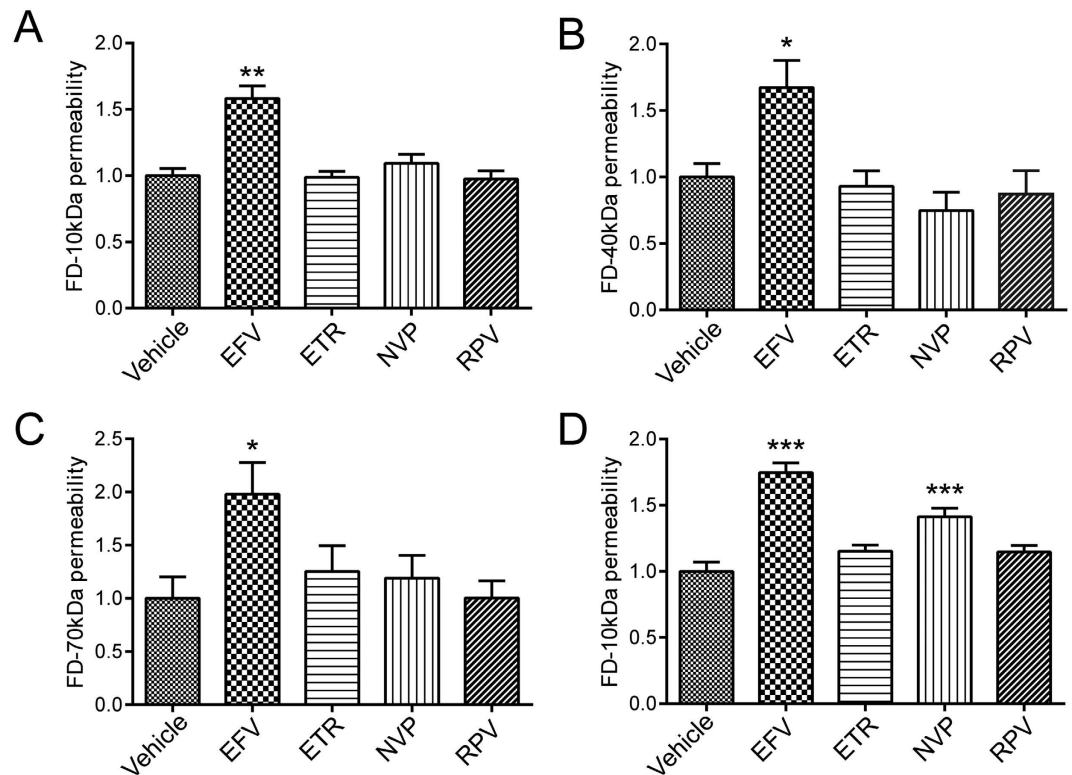


Figure 1. Impact of NNRTIs on endothelial permeability. hCMCEC (A–C) and human primary brain endothelial cells (D), grown to confluence on Transwells, were incubated with vehicle (DMSO), Efavirenz (Efa), Etravirine (ETR), Nevirapine (NVP) or Rilpivirine (RPV) for 48 h. Culture media in the apical compartment of the Transwell system was replaced with medium containing FD of 10 kDa (A and D), 40 kDa (B) or 70 kDa (C). Basolateral levels of FD were assayed 90 min post exposure. Data are mean \pm SEM, expressed as fold increase over vehicle control; three independent experiments, each with $n = 4$; * $p < 0.05$ vs. Vehicle; ** $p < 0.01$ vs. Vehicle; *** $p < 0.001$ vs. Vehicle.

a general reduction in expression level of this protein (Fig. 3A and B; arrows). Confirming these results, Efavirenz at 10 μ M and 15 μ M (but not other NNRTIs) decreased claudin-5 immunoreactivity and its presence at cell-cell junctions in primary human brain endothelial cells (Fig. 3C). These results demonstrate that in addition to a reduced expression, Efavirenz treatment affects subcellular localization of claudin-5 at TJs.

ER stress inhibition protects against Efavirenz-induced a decrease in claudin-5 expression, but not endothelial dysfunction. To identify the mechanisms of Efavirenz-induced claudin-5 downregulation, we first evaluate mRNA levels in cells exposed to increasing doses of this drug. While small changes in claudin-5 mRNA were detected (Fig. 4A), they did not correlate with the observed changes at the protein level. Specifically, a decrease in claudin-5 mRNA was observed in cells exposed to Efavirenz at 1 μ M, i.e., the levels of the drug which increased claudin-5 protein level. In addition, 10 μ M Efavirenz elevated claudin-5 mRNA (Fig. 4A); however, the same dose of Efavirenz consistently decreased claudin-5 protein expression (Figs 2 and 3). These results suggested a post-transcriptional mechanism of Efavirenz-induced alterations of claudin-5 expression.

We previously demonstrated that Efavirenz can induce ER stress²⁵, which is a cellular response that can affect protein expression, via at least two ER sensors: PERK and IRE1 α . Therefore, we evaluated whether induction of ER stress is involved in Efavirenz-induced alterations of claudin-5 expression. hCMCEC were pretreated with several ER stress inhibitors (GSK2606414, PERK inhibitor; STF-083010, IRE1 α inhibitor; 4 μ 8c, IRE1 α inhibitor; or 4-phenylbutyrate [4PBA] a broad inhibitor/chaperone) for 6 h, followed by treatment with Efavirenz for 48 h. As indicated in Fig. 4B, claudin-5 expression was restored to the control levels by 4 μ 8c and 4PBA. However, treatment with 4 μ 8c disrupted endothelial barrier function, and 4PBA was not effective in protecting against Efavirenz-induced disruption of endothelial permeability (Fig. 4C). These results indicate that ER stress inhibition can restore protein levels of claudin-5; however, this recovery does not fully extend to endothelial integrity. To explain this discrepancy, we observed that pretreatment with 4 μ 8c or 4PBA failed to restore claudin-5 staining at cell junctions (Fig. 4D, arrows).

TJ protein levels are critical for TJ assembly and the barrier function, however an additional factor that may affect endothelial permeability is their phosphorylation. It has been demonstrated that claudin-5 phosphorylation results in an increase in BBB permeability, and that this modification can be in part mediated by Rho kinases⁵⁷. Therefore, we analyzed phosphorylation levels of claudin-5 by western blotting in cells exposed to Efavirenz. The results indicated that Efavirenz resulted in a significant increase in claudin-5 phosphorylation, which was

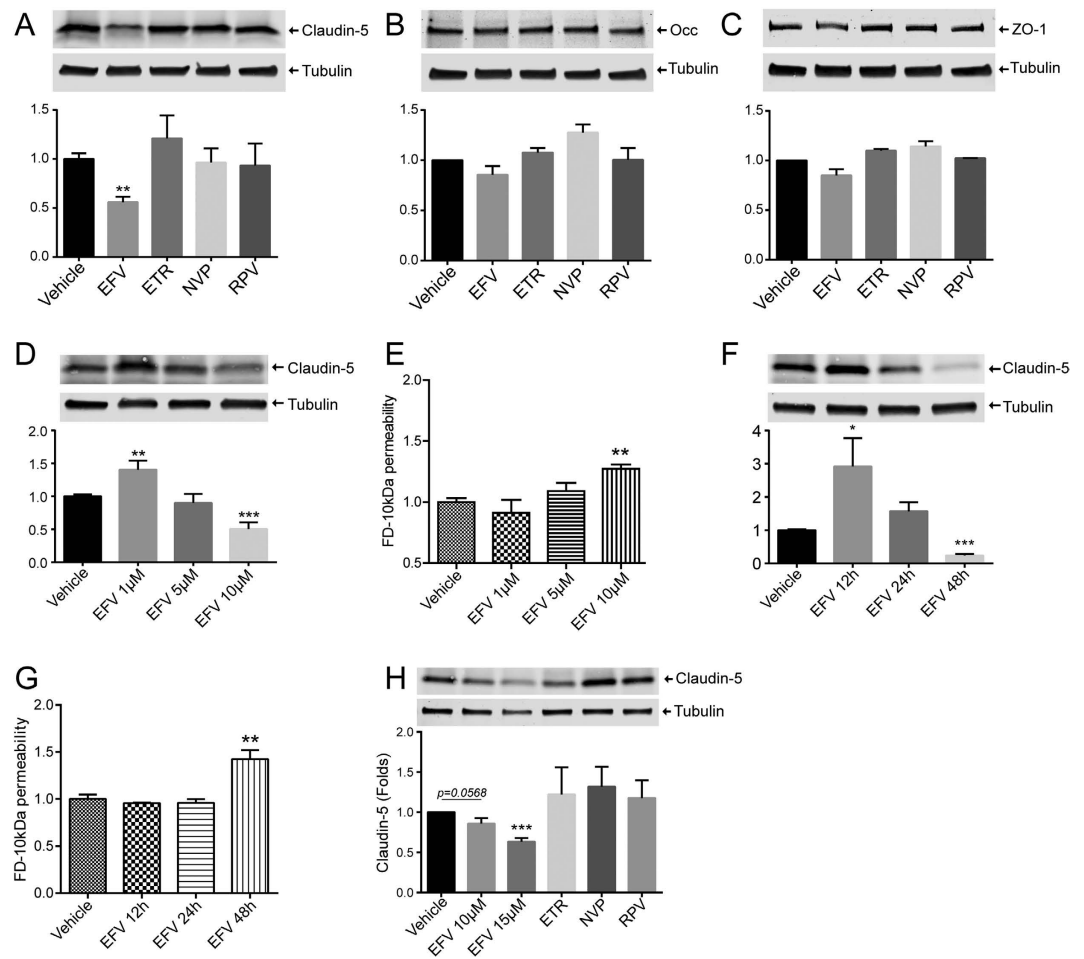


Figure 2. Impact of NNRTIs on tight junction protein expression. hCMEC (A–G) and human primary brain endothelial cells (H) were grown to confluence, followed by exposure to vehicle (DMSO), Efavirenz (Efa), Etravirine (ETR), Nevirapine (NVP) or Rilpivirine (RPV) for 48 h. Expression of claudin-5 (A,D,E,H), occludin (B), and ZO-1 (C) was assessed by western blotting. Dose-dependent effects of Efavirenz on claudin-5 levels (D,H) and endothelial permeability (E). Time-dependent impact of Efavirenz on claudin-5 levels (F) and endothelial permeability (G). Presented blots are cropped from the originals, full size blots available in Supplementary Fig. S1. Data are mean \pm SEM, expressed as fold increase over vehicle control; three or four independent experiments, each with $n=4$. * $p < 0.05$ vs. Vehicle; ** $p < 0.01$ vs. Vehicle; *** $p < 0.001$ vs. Vehicle.

not restored by pretreatment with 4 μ M c or 4PBA (Fig. 4E). This indicated that while 4PBA prevents Efavirenz mediated reduction in claudin-5 proteins levels, phosphorylation levels remain high, the effect that correspond with disrupted barrier function.

Treatment with Efavirenz, but not other NNRTIs, disrupts TJs in an animal model. Following the *in vitro* analyses, we next evaluated whether Efavirenz-induced alterations of TJ proteins occur *in vivo* in an animal model. Mice were gavaged with either vehicle, Efavirenz, Etravirine, or Rilpivirine for 30 days. Afterward, brains were harvested, the microvessels were isolated and analyzed by immunofluorescence for the expression and localization of claudin-5, occludin, and ZO-1 (Fig. 5A and B). Among all NNRTIs used, only treatment with Efavirenz resulted in reduction of claudin-5 and ZO-1 immunoreactivity. Quantitative analysis of signal intensity by mean fluorescence intensity (MFI) demonstrated a significant decrease in claudin-5 and to a lesser degree in ZO-1 in mice exposed to Efavirenz as (Fig. 5C). These changes were associated with disrupted claudin-5 colocalization with ZO-1 (Fig. 5A) and occludin (Fig. 5B). These results indicate that Efavirenz-induced TJ disruption occurs *in vivo* in a physiologically relevant treatment regimen.

Efavirenz disrupts TJ integrity in EcoHIV/NDK-infected brains. Given that ARVd are typically used in HIV-infected individuals, we next compared the impact of Efavirenz on TJ integrity in mice infected with a chimeric HIV virus specifically adapted for mice, EcoHIV/NDK. To target the brain for infection, the virus was infused into the internal cerebral artery⁵⁸, mimicking the initial stages of HIV brain infection in which the blood-borne virus enters the brain via the BBB. EcoHIV inoculation resulted in a preferential infection of the ipsilateral hemisphere, which corresponds to the site of virus infusion (Fig. 6A). The infection was confirmed by

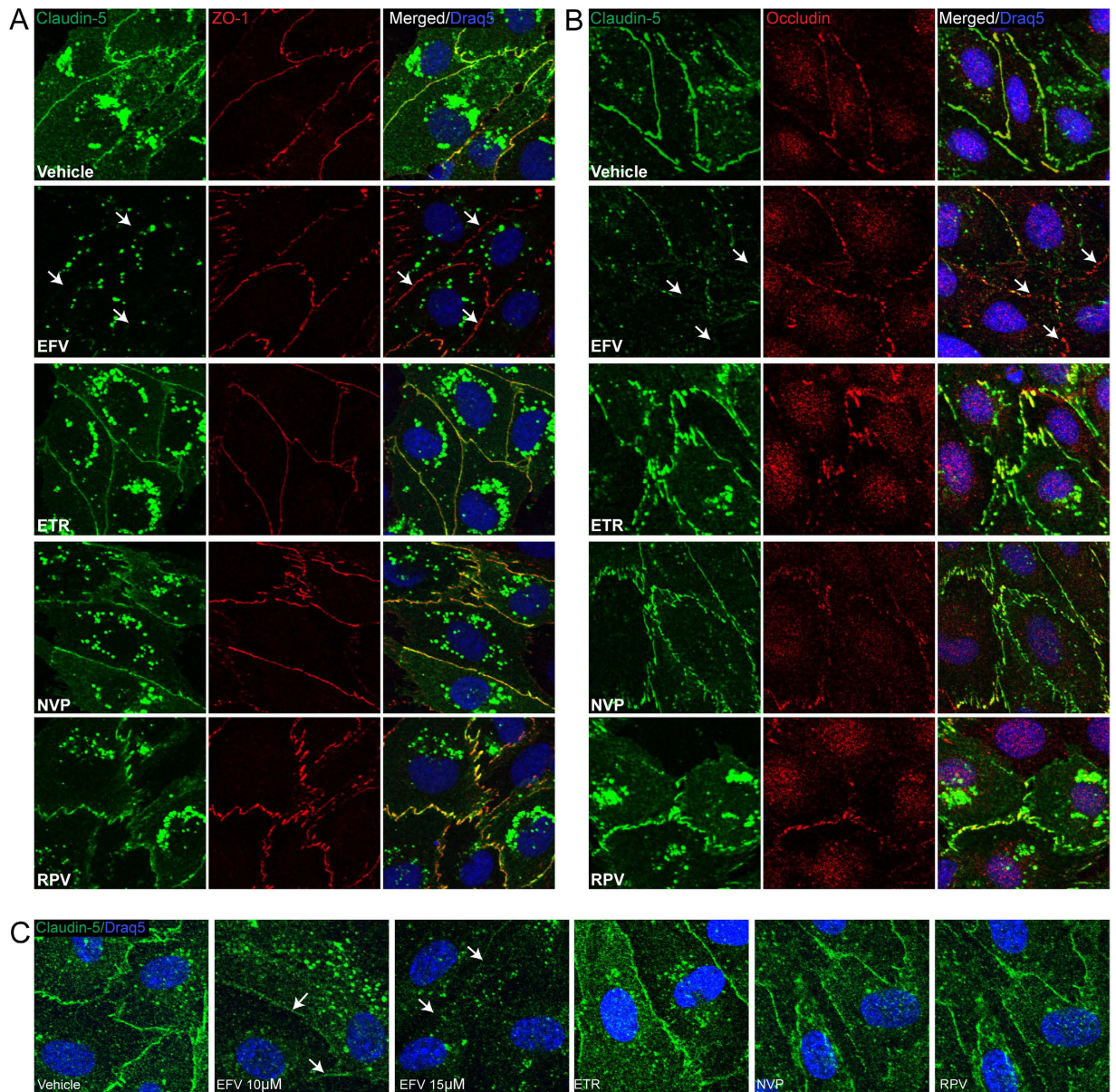


Figure 3. Treatment with Efavirenz, but not with other NNRTIs, decreases claudin-5 immunoreactivity and localization. hCMEC were grown on coverslips to confluence, exposed to NNRTIs as in Fig. 1, and immunostained for claudin-5 (green), ZO-1 (red), or occludin (red). Draq5 (blue) visualizes nuclei. Left and middle columns in **A** and **B** are staining for specific tight junction proteins. The right column in **(A)** is colocalization of claudin-5 with ZO-1, and the right column in **(B)** is colocalization of claudin-5 with occludin. **(C)** Localization of claudin-5 in primary human brain endothelial cells. Arrows indicate discontinuous, absence of claudin-5 immunoreactivity and lack of ZO-1 or Occludin colocalization. EFV: Efavirenz; ETR: Etravirine; NVP: Nevirapine; RPV: Rilpivirine.

in situ PCR, which detected EcoHIV-infected cells mainly in the striatum (Fig. 6B). Seven days post infection, mice were treated for 30 days with Efavirenz or vehicle. Then, brain microvessels were isolated and immunostained for occludin (images not shown), claudin-5, and ZO-1 (Fig. 6C). The expression values of TJ proteins were calculated as MFI.

The infection with EcoHIV did not alter the MFI values for claudin-5 and occludin; however, ZO-1 levels were diminished as compared to mock infection (Fig. 6C and D). Treatment with Efavirenz markedly decreased claudin-5 levels in both animal groups, did not alter occludin levels, and diminished ZO-1 expression only in mock-infected mice. In addition, a reduction in colocalization of claudin-5 with occludin was identified using the Mander's coefficient in both mock- and EcoHIV-infected mice (Fig. 6E). Colocalization of claudin-5 with ZO-1 was decreased only in mock-infected mice.

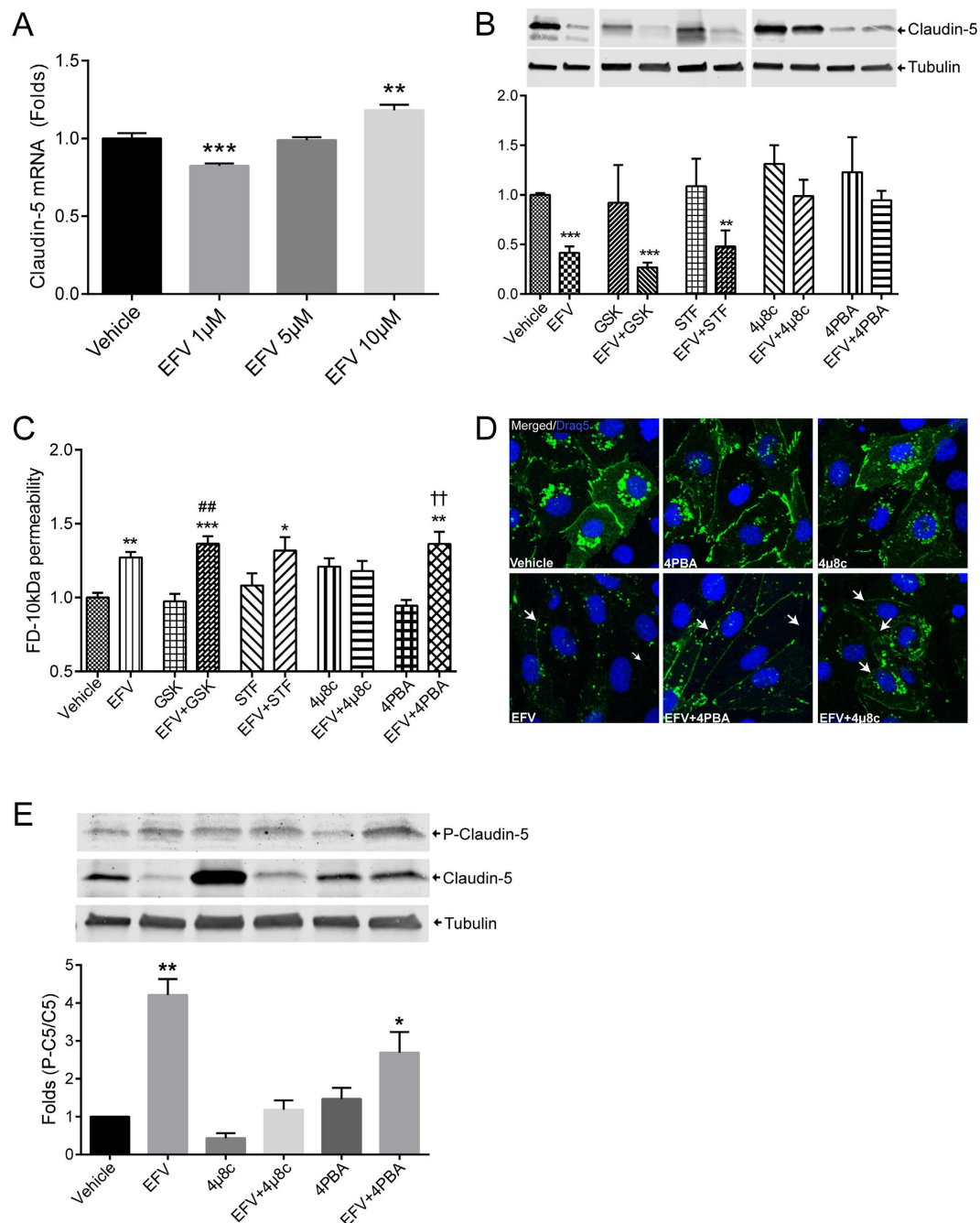


Figure 4. Inhibition of ER stress restores Efavirenz-induced alterations of claudin-5 protein levels but not claudin-5 phosphorylation and disrupted endothelial permeability. (A) Dose-dependent effects of Efavirenz on claudin-5 mRNA levels as analyzed by real-time PCR. (B) Cells were pretreated with various ER stress inhibitors for 6 h before a 48 h exposure to 10 μ M Efavirenz, followed by immunoblotting for claudin-5 protein expression. Tubulin was assessed as house-keeping reference. (C) Cells were treated as in (B) and endothelial permeability was evaluated using FD-10kDa dye transfer as in Fig. 1. (D) Cells were pretreated with selected inhibitors of ER, followed by exposure to Efavirenz as in (C), and followed by staining for claudin-5 immunoreactivity (green). Draq5 (blue) visualizes nuclei. Arrows indicate discontinuous or absence of claudin-5 immunoreactivity. (E) Claudin-5 phosphorylation levels in cells exposed as in (D). Graphs represent ratio of phosphorylated claudin-5 (P-Claudin-5) compared to total claudin-5 levels. Presented blots are cropped from the originals, full size blots available in Supplementary Fig. S1. Data are mean \pm SEM, expressed as fold increase over vehicle control; three or four independent experiments, each with $n = 4$. GSK: GSK2606414; STF: STF-083010; 4PBA: 4-Phenylbutyrate; EFV: Efavirenz. * $p < 0.05$ vs. Vehicle; ** $p < 0.01$ vs. Vehicle; *** $p < 0.001$ vs. Vehicle; ## $p < 0.01$ vs. GSK; †† $p < 0.01$ vs. 4PBA.

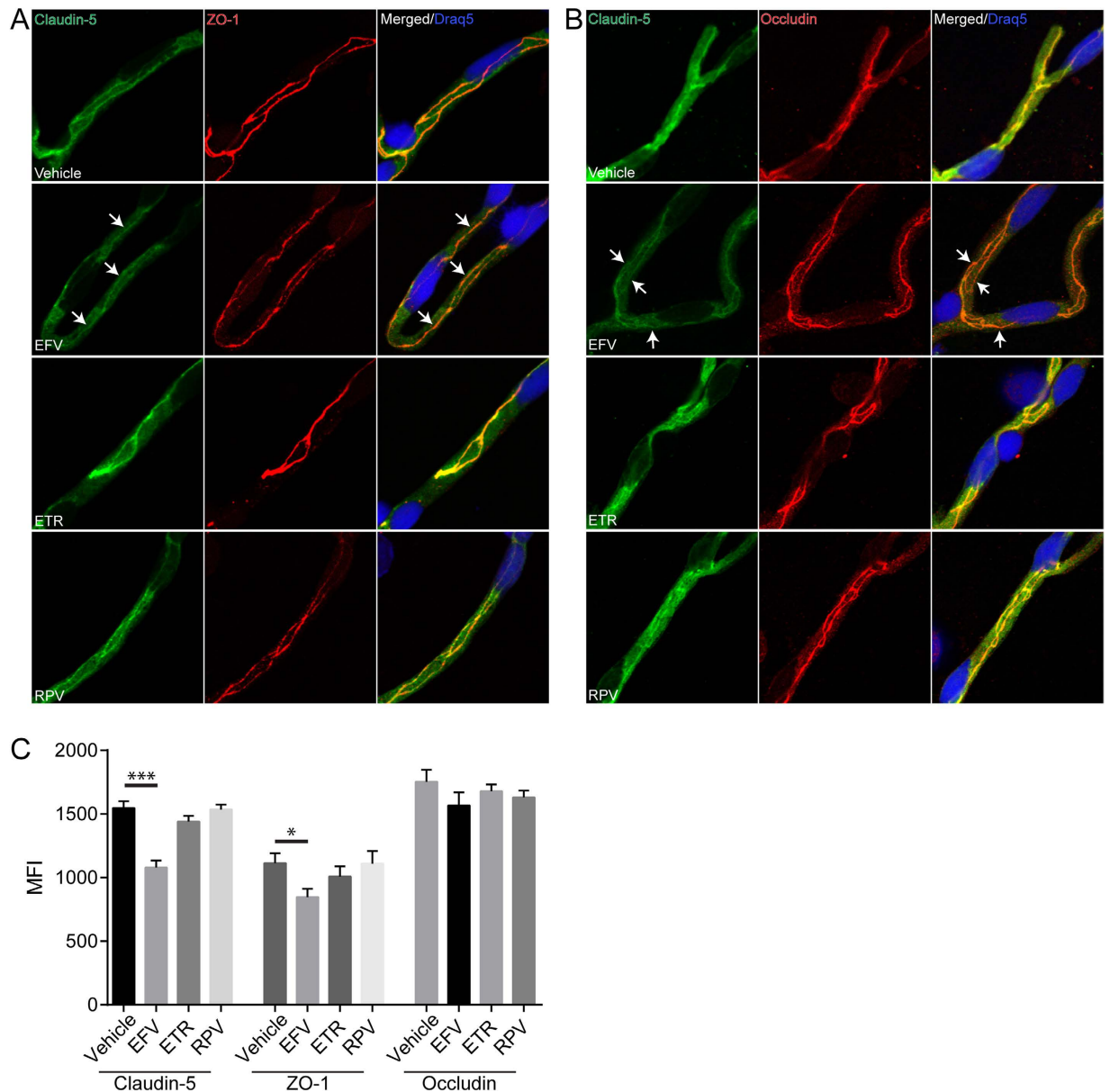


Figure 5. Treatment with Efavirenz, but not other NNRTIs, affects claudin-5 immunoreactivity and localization in brain microvessels. Mice were treated with various NNRTIs or vehicle for 30 days as described in the Materials and Methods. Claudin-5 (green), ZO-1 (red), and occludin (red) were analyzed by immunostaining in isolated brain microvessels. Nuclei were stained with Draq5 (blue). Left and middle columns in **A** and **B** are staining for specific tight junction proteins. The right column in (**A**) is colocalization of claudin-5 with ZO-1 and the right column in (**B**) is colocalization of claudin-5 with occludin. Arrows indicate discontinuous, absence of claudin-5 immunoreactivity and lack of ZO-1 or Occludin colocalization. (**C**) Quantification of mean fluorescence index (MFI) signal for tight junction proteins analyzed in isolated microvessels. Data obtained from 3 mice per group, 5–7 microvessels per mice. * $p < 0.05$; *** $p < 0.001$. EFV: Efavirenz; ETR: Etravirine; RPV: Rilpivirine.

Efavirenz treatment increases BBB permeability and amplifies stroke severity in HIV-infected brains. Taking into consideration that TJs play a primordial role in maintaining BBB integrity, we evaluated the impact of NNRTIs on the BBB permeability. Animals were treated with NNRTIs as in Fig. 6, followed by intraperitoneal injection with sodium fluorescein (NaF), which was allowed to circulate for 20 min. Mice were then euthanized; blood was collected via cardiac puncture, and animals were perfused with saline. Brains were carefully harvested and processed for NaF quantitation. Treatment with Efavirenz, but not with other NNRTIs, induced a significant increase in NaF levels in the brains, indicating disrupted barrier function of the BBB (Fig. 7A). These results demonstrate that the disruption of TJ integrity caused by Efavirenz has functional implications on BBB permeability.

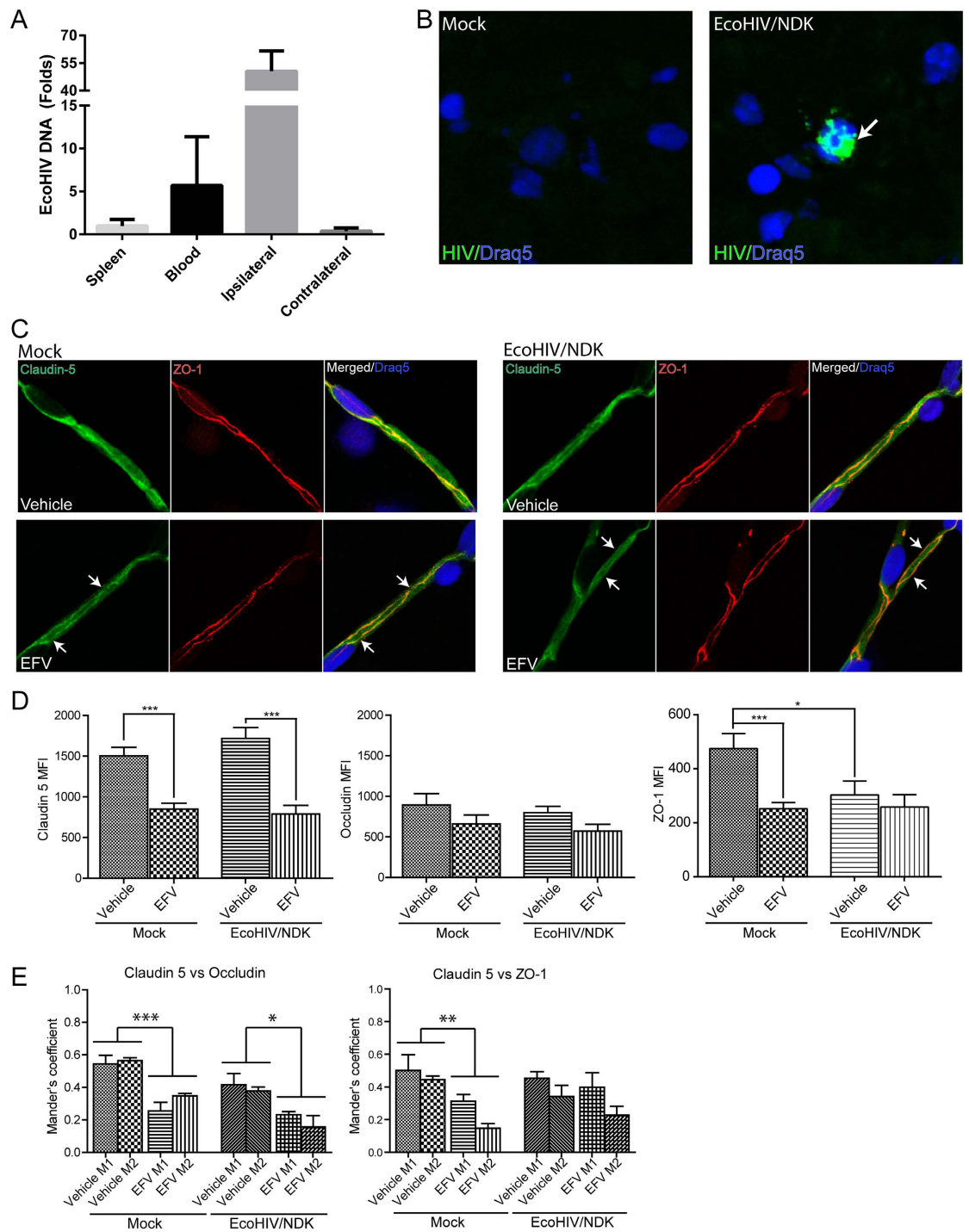


Figure 6. Tight junction protein expression and colocalization in EcoHIV/NDK-infected brains. Mice were infected with the mouse adapted strain EcoHIV/NDK infused into the common carotid artery. **(A)** Real-time PCR analysis of HIV DNA content one week post infection. Bars represent fold changed compared to spleen HIV DNA content ($n = 5$). **(B)** *In situ* PCR analysis of HIV presence in brain sections of mock or EcoHIV/NDK infected mice. Positive HIV amplification is indicated in green (arrow). Nuclei are stained with DraQ5 (blue). **(C)** Immunofluorescence of tight junction proteins in brain microvessels isolated from mock (left panel) or EcoHIV/NDK-infected (right panel) mice and treated with vehicle or Efavirenz (10 mg/kg for 30 days). Slides were immunostained for claudin-5 (green) and ZO-1 (red); DraQ5 (blue) was used to stain nuclei. Arrows indicate discontinuous, absence of claudin-5 immunoreactivity and lack of ZO-1 colocalization. **(D)** Mean fluorescence index analysis of tight junction protein staining in isolated brain microvessels as in **(C)**. Claudin-5, ZO-1, and occludin immunoreactivity was analyzed. **(E)** Analysis of colocalization of claudin-5 with ZO-1 or claudin-5 with occludin using the Mander's coefficient. **(C–E)** Data obtained from 5 mice per groups, 5–9 microvessels per mice. Data are mean \pm SEM. Analysis was performed using Image J and JACoP plugin. EFV: Efavirenz. * $p < 0.05$; ** $p < 0.01$; *** $p < 0.001$.

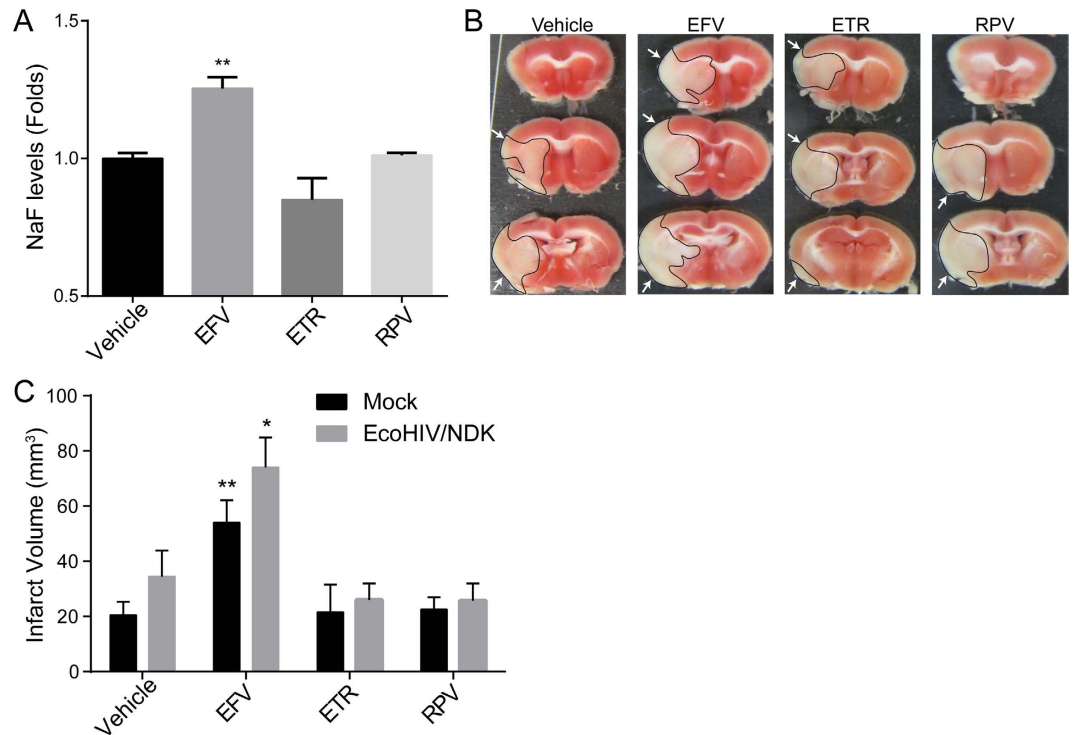


Figure 7. Efavirenz increases BBB permeability and stroke tissue injury. (A) Quantification of BBB permeability. Mice were treated for 30 days with either vehicle or NNRTIs as described in the Material and Methods. Translocation of sodium fluorescein (NaF) from plasma into the brain parenchyma was used as the indicator of BBB integrity. Data are mean \pm SEM, expressed as fold change compared to vehicle, $n = 5$ per group. To analyze infarct volume, mice were either mock or EcoHIV/NDK infected and treated as in (A). Brains were stained with TTC 24 h after a 60 min occlusion of the middle cerebral artery occlusion (MCAO). (B) Representative images of infarct areas in brain slices from NNRTI-treated mock-infected mice. Infarct areas are highlighted and indicated by arrows. (C) Quantification of total infarct volume from all animal groups. Data are mean \pm SEM, $n = 4$ –7 animals per group. * $p < 0.05$ vs. Vehicle; ** $p < 0.01$ vs. Vehicle.

We next evaluated whether exposure to specific NNRTIs contributes to the development of stroke during HIV infection. HIV-infected patients are known to have a higher risk of stroke, which is often also more severe. Furthermore, stroke development and severity is exacerbated by a disrupted BBB⁵⁰.

Mice were infected with EcoHIV and treated with NNRTIs as in Fig. 6, followed by induction of stroke by the middle cerebral artery occlusion (MCAO) for 60 min and reperfusion for 23 h⁵⁹. Afterward, brains were harvested, sliced, and stained to analyze infarct volume. Among all tested NNRTIs, only Efavirenz treatment induced a significant increase in stroke severity when compared to vehicle. This phenomenon was observed both in mock and EcoHIV-infected mice (Fig. 7B and C). While there was a trend for a larger infarct volume in infected animals, the differences between the groups were below the threshold of statistical significance. These results indicate that while HIV is a potential contributor to stroke, Efavirenz has a highly significant impact on stroke severity, almost doubling infarct volume when compared to vehicle controls.

Discussion

The suppression of HIV replication using ARVd is essential in maintaining the health of seropositive patients. However, given that patients require antiretroviral therapy for the rest of their lives, drug toxicity is an important factor to take into consideration to prevent complications, and decrease the potential of exacerbating secondary diseases. Several publications demonstrated that selected ARVd used in the treatment of HIV have serious side effects which can affect patient health outcome. In addition, while HAART can suppress viral replication below detectable levels, there is a continuous presence of circulating viral proteins that alone can contribute to disease and lower the threshold of ARVd toxicity⁶⁰.

While several categories of ARVds exist and are used in HIV-infected patients, we focused on toxicity of NNRTIs, selecting drugs from the first and second design generation that are currently in use in clinics. Even though Efavirenz was recently removed from the initial treatment option in the US, it is still part of the first NNRTI based regimen recommended by the WHO, and remains commonly used worldwide. Second generation NNRTIs have also been included in this study to evaluate cerebrovascular effects and safety of these drugs. We, and others, reported that Efavirenz induces ER stress and affects the autophagy pathway^{23–25}, which are likely to affect other pathways and impact cell functions in biological systems. In the current study, we investigated the toxicity of Efavirenz, as well as Etravirine, Nevirapine, and Rilpivirine, by focusing on one of the primary roles of brain endothelial cells, namely the integrity of the BBB.

The structure of the BBB relies on the function of multiple cells, namely endothelial cells, pericytes, and astrocytes. While conditions affecting any of those cells can compromise the integrity of this barrier, we focused our investigation on brain microvascular endothelial cells given their central role in the formation and regulation of the BBB. Our results demonstrate that at physiologically relevant concentrations, of all of the NNRTIs tested, only Efavirenz affected endothelial integrity, leading to an increase in permeability. While we observed a slight increase in permeability of primary brain endothelial cells exposed to Nevirapine, none of the other tests performed confirmed endothelial toxicity of this drug. The barrier function is highly reliant on the formation of TJs, composed especially claudin-5, ZO-1, and occludin, which were included in the present study. Claudin-5 was demonstrated to be an important contributor to BBB integrity⁶¹ and its upregulation correlates with a protective effect against CNS tissue injury⁶². Similar observations have been made for ZO-1 and occludin both *in vitro* and *in vivo*^{62–65}. In our model system, exposure to Efavirenz selectively decreased the levels of claudin-5. These effects were dose- and time-dependent, and were observed both *in vitro* (in two different model systems) and *in vivo*. Efavirenz also had an impact on intracellular localization of this protein, with the prominent effect on removing claudin-5 from cell-cell junctions. In contrast, no changes in expression levels or localization were observed for occludin in our model systems. ZO-1 levels were not affected *in vitro*; however, they decreased upon Efavirenz administration in an animal model. This observation is important as it demonstrates that *in vitro* drug toxicity assays do not fully reproduce responses in more complex biological systems. Treatment with Efavirenz also disrupted the integrity of the BBB *in vivo*, which is consistent with the role of claudin-5 in maintaining the BBB barrier function⁶⁶.

We next sought to identify the mechanisms of claudin-5 disruption. Given our previous observations that Efavirenz induced ER stress in brain endothelial cells, we investigated the role of this process in alterations of claudin-5 expression and localization. This line of investigation is consistent with the reports on the role of ER stress in vascular dysfunction in coronary disease^{67,68}, diabetic retinopathy⁶⁹ and, several other processes involving endothelium^{70,71}. While the role of claudin-5 in maintaining vessel integrity is well established, limited data is available on the impact ER stress on integrity of claudin-5 and other TJ proteins^{51,72–74}.

We demonstrated previously that the PERK and IRE1 α pathways are involved in Efavirenz-induced ER stress. Based on these results, several inhibitors were employed in the present study to explore the link between ER stress, claudin-5, and disrupted endothelial permeability. We identified two inhibitors, namely 4 μ 8c and 4PBA, which prevented Efavirenz-induced alterations of claudin-5 expression; however, they did not restore endothelial barrier function. Regarding 4 μ 8c, given that it alone resulted in an increase in endothelial permeability, it is reasonable to assume that an off target effect could be at play. On the other hand, 4PBA restored the total levels of claudin-5 in Efavirenz-treated cells; however, immunostaining pattern exhibited a preserved diminished intensity and discontinuity at cell-cell junctions. In addition, 4PBA pretreatment did not restore Efavirenz-induced alterations of claudin-5 phosphorylation, a process that is influenced by Rho kinases and leads to a decrease in TJ tightness^{75,76}. To support this notion, it has been shown that Efavirenz can increase cytoplasmic calcium levels, which has been linked to Rho kinase activation⁷⁷. In addition, HIV-1 is known to activate RhoA⁵⁷, further contributing to BBB disruption in seropositive patients and potentially increasing neuroinvasion.

In light of the concerns that ARVd can contribute to neurotoxicity in HIV-1 infection, we employed a mouse adapted strain of HIV called EcoHIV/NDK in which the viral gp120 protein was replaced with gp80 for the tropism to mouse cells^{78–81}. To mimic a natural route of infection while promoting CNS entry, virus was inoculated by infusion via the internal cerebral artery. This technique induces a strong preference for CNS infection in the infused hemisphere. Compared to mock infection, we did not observe any differences in claudin-5 expression in either the vehicle- or Efavirenz-treated group. Nevertheless, brain infection with EcoHIV/NDK diminished expression of ZO-1 intensity in brain microvessels. This decreased expression corresponded to the impact of Efavirenz treatment, and no further reduction was observed in the HIV plus Efavirenz group as compared to HIV or Efavirenz alone. The link between ZO-1 and HIV has previously been identified and was associated, at least in part, to the toxic effect of HIV Tat protein^{82–85}.

While several diseases are associated with HIV infection, cerebrovascular events are among the leading causes of mortality^{86–88}. Therefore, we also evaluated the impact of NNRTI treatment on stroke in both mock or HIV infected mice. Our novel results indicate that Efavirenz treatment significantly increased stroke severity, inducing a two-fold increase in tissue damage as compared to controls. These results are consistent with the impact of this drug on claudin-5 expression and BBB integrity. HIV infection lead to a small increase in infarct volume in all treatment groups; however, it was below the threshold of significance.

In summary, our findings indicate that while HAART is an integral part of HIV treatment in seropositive patients, the choice of drugs used in the treatment regimen is crucial in preventing toxicity. Indeed, selected NNRTIs, such as Efavirenz, can deteriorate treatment outcome, especially in people subjected to cerebrovascular disease.

Material and Methods

Cell culture and virus stock preparation. Human cerebral microvascular endothelial cells (hCMEC; hCMEC/D3 cell line) were obtained by immortalizing human brain microvascular cells⁸⁹. The cells are very well characterized and have been widely used in the literature, including our studies on ARVd toxicity⁸⁹. The cells were cultured in EBM-2 medium (Lonza) supplemented with VEGF, IGF-1, EGF, basic FGF, hydrocortisone, ascorbate, gentamycin, and 0.5% fetal bovine serum (FBS, Lonza) in cell culture dishes coated with rat-tail collagen I (BD Bioscience) in 5% CO₂ humid incubator at 37 °C. HEK293T/17 cells (ATCC) were cultured in DMEM medium supplemented with 10% FBS. Primary human brain endothelial cells (Cell Systems) were cultured in CSC complete medium on dishes coated with CSC attachment factor (all from Cell Systems).

Chimeric HIV virus EcoHIV/NDK was used for mouse infection. EcoHIV/NDK was generated by replacing the viral gp120 protein with gp80 for the ecotropic moloney murine leukemia virus⁷⁸. The viral plasmid was a kind gift from Dr. David Volsky (Icahn School of Medicine at Mt. Sinai, New York, NY). Viral stocks were

prepared by transfecting HEK 293 T/17 cells with the plasmid using lipofectamine 2000 (Invitrogen). Viral concentration in the filtered supernatant was quantified using p24 ELISA kit (Zeptomatrix).

Drugs and inhibitor treatment. Exposure to NNRTIs was conducted in serum-free and antibiotic-free media for 48 h at the following concentrations: Efavirenz (1, 5, 10, and 15 μM), Etravirine (1.6 μM), Rilpivirine (0.5 μM), and Nevirapine (7.8 μM). These concentrations reflect physiological plasma concentrations of the drugs^{90,91}. Regarding Efavirenz levels, both 10 and 15 μM are relevant to human exposure. While the mean plasma concentration of Efavirenz can vary from 3.17 to 12.67 μM in the majority of patients, a proportion of them (up to 14% in some studies) exhibit even higher concentrations⁹¹. ARVds were acquired from the NIH AIDS Reagent Program (NIAID, Germantown, MD).

Activation of ER stress was blocked using the following inhibitors: GSK2606414 (7 μM), STF-083010 (10 μM), 4 μ 8c (3 μM) (All EMD-Millipore) and 4-phenylbutyrate (2 mM, Sigma-Aldrich). Pre-exposure to ER stress inhibitors was initiated 6 h before NNRTI treatment.

Animal treatment, infection with EcoHIV/NDK, and the middle cerebral artery occlusion procedure.

All animal procedures were approved by the University of Miami Institutional Animal Care and Use Committee in accordance with National Institutes of Health (NIH) guidelines and performed in accordance with the relevant guidelines and regulations. Male C57BL/6 J mice (Jackson Laboratories) were allowed to acclimatize to the animal facility for one week with free access to food and water. They were then infused with EcoHIV/NDK (200 ng of p24) into the internal carotid artery using a method previously described^{58,92,93}. Control animals received saline. Administration of NNRTIs started seven days post infection, and lasted for 30 days. Mice were gavaged daily with either 12.5% DMSO in saline (control), 10 mg/kg Efavirenz, 6.6 mg/kg Etravirine, or 0.42 mg/kg Rilpivirine (NIH AIDS Reagent Program). Afterward, mice were sacrificed for microvessels isolation or were used for *in vivo* BBB permeability assay or stroke studies.

Stroke was induced following the drug administration by the middle cerebral artery occlusion (MCAO) as described^{59,94}. Briefly, occlusion was performed by insertion a silicone coated suture (Doccol) into the common cerebral artery and blocking blood flow to the middle cerebral artery for 60 min. Afterward, the suture was removed and blood flow restored for 23 h. Brains were harvested, sliced using a 1 mm brain matrix (Braintree Scientific) and stained with 2,3,5-triphenyltetrazolium chloride (TTC, ThermoFisher). The images were captured using a digital camera and infarct volume was analyzed using Image J.

Permeability assays. *In vitro* endothelial permeability assays were performed in 12 wells, 0.4 μm Transwells plates (Corning) using either hCMEC (seeded at 6×10^4 cells per insert) or human primary brain endothelial cells (seeded at 5×10^4 cells per insert). Medium was changed every 48 h and monolayer formation was monitored using trans-epithelial electrical resistance. Seven days after seeding, medium was changed in the upper chamber for one containing treatment factors. Following exposure, media was replaced with Hanks balanced salt solution in both chambers; however, fluorescently tagged dextran (10, 40 or 70 kDa) was added to the upper chamber at the concentration of 0.5 mg/ml. Fluorescent marker translocation was analyzed after 90 min incubation by transferring 100 μl aliquots from the lower chamber to a 96 well plaque and reading fluorescence at 485 nm (Ex) and 525 nm (Em).

In vivo BBB permeability assay was performed using sodium fluorescein (NaF) as described before⁹⁵. Briefly, mice were injected intraperitoneally with 200 μl of 10% NaF solution, which was allowed to circulate for 20 min. Mice were euthanized, blood was collected via heart puncture, and animals were perfused using normal saline. Brain hemispheres were thoroughly homogenized in PBS using a tissuelyser system (Qiagen) and cleared of debris by centrifugation. Sample protein concentration was measured to normalize the results. Proteins were precipitated with 100% TCA (Sigma-Aldrich), followed by centrifugation. Supernatants were mixed with 0.05 M sodium tetraborate buffer and NaF fluorescence was measured in the supernatants using a fluorescent plate reader (485 nm Ex, and 525 nm, Em). In addition to the brain, plasma NaF levels were assessed to control for injection variation.

Immunoblotting and immunostaining. Cells were exposed to vehicle or NNRTIs in 100 mm dishes, washed, and lysed in RIPA buffer (Santa Cruz Biochemical) containing protease/phosphatase inhibitors (Cell Signaling) 48 h post-exposure, unless otherwise stated. Protein concentration was assessed using a BCA protein assay (Pierce), and 20 μg of protein per sample was loaded on a TGX 4–20% gradient gel (Biorad). Transfer was performed on a nitrocellulose membrane using a Trans-blot Turbo system (Biorad). Afterward, membranes were blocked in 4% BSA in TBS. Primary antibodies were incubated for 1.5 h at room temperature in blocking buffer supplemented with 0.1% Tween-20 and applied at the following concentrations: 1:1000 (claudin-5, Cell Signaling (Rb) and Invitrogen (Ms); claudin-5 (P-Y217), Abcam; ZO-1, Invitrogen; occludin, Invitrogen) or 1:10,000 (Tubulin, Sigma). Membranes were imaged in a Licor CLX imaging system with the secondary antibodies diluted at 1:20 000 (anti-rabbit 800CW and anti-mouse 680RD, Licor). Signal quantification was performed using Image Studio 4.0 software (Licor).

Immunostaining was performed on cultured cells or isolated microvessels, which were heat-fixed on slides and processed as previously described²⁵. Samples were stained with rabbit antibodies against claudin-5 (Abcam) and ZO-1 (Cell Signaling), or with mouse antibodies against claudin-5 (Invitrogen) and occludin (Invitrogen). Alexa-488 and -594 secondary antibodies (Invitrogen) were used for target detection; DRAQ5 (Cell Signaling) was employed to stain cell nuclei. Imaging was performed on an Olympus Fluoview 1200 confocal microscope with a 60x oil immersion lens, and analyzed using ImageJ software.

HIV detection by *in situ* PCR. *In situ* PCR was used to detect cells infected with HIV. Brains of mice either mock- or EcoHIV/NDK infected were harvested 1 week post infection, flash-frozen in liquid nitrogen,

sliced at 10 μm , and kept at -80°C until analysis. Slides were processed for *in situ* PCR as described⁹⁶. Briefly, sections were fixed in 4% paraformaldehyde for 4 h at room temperature and then digested using protease K at 5 $\mu\text{g}/\text{ml}$ for 12 min at 25°C . The enzyme was inactivated by a 95°C incubation for 2 min. PCR mixture was prepared as described⁹⁶, but modified for primers labeled with Alexa-594 to directly detect the PCR product. The following primers were used: NDK_F 5'-ALEXA 594-GGACCACAGGCTACACTAGAAG; NDK_R 5'-CAGCCAAAACCTCTTGCTTTATG. Slide PCR was performed using an Xmatrx mini (Biogenex) cycler and Frame-seal slide chambers (Biorad). Slides were fixed at 92°C for 1 min, stained with DRAQ5, and washed twice in 2x saline sodium citrate buffer. Imaging was performed as described in the section on immunofluorescence.

Real-time PCR. mRNA was isolated using RNeasy mini kit (Qiagen) and reverse transcribed by reverse transcription system (Promega) according to manufacturer's instructions. Real time PCR was performed using an Applied Biosystem 7500 System and primers and probes for claudin-5, ZO-1 and occludin (ThermoFisher). GAPDH mRNA level was assessed in duplication for data normalization.

Tissue detection of EcoHIV/NDK was performed 1 week post infection. Tissue was harvested and processed using All Prep DNA/RNA isolation kit (Qiagen). RNA was reverse transcribed as described above. HIV detection was then conducted using the following primers and probe: NDKgag_F 5'-GACATAAGACAGGGACCAAAGG; NDKgag_R 5'-CTGGGTTTGCATTTTGGACC; NDKgag_Probe 5'-AACTCTAAGCCGAGCAAGCTTCAC. Normalization was conducted based on GAPDH for RNA or mouse HBB for DNA⁸⁰.

References

- Vance, D. E. Aging with HIV: clinical considerations for an emerging population. *Am J Nurs* **110**, 42–47; quiz 48–49, doi: 10.1097/01.NAJ.0000368952.80634.42 (2010).
- Costagliola, D. Demographics of HIV and aging. *Curr Opin HIV AIDS* **9**, 294–301, doi: 10.1097/COH.0000000000000076 (2014).
- Bhatia, N. S. & Chow, F. C. Neurologic Complications in Treated HIV-1 Infection. *Curr Neurol Neurosci Rep* **16**, 62, doi: 10.1007/s11910-016-0666-1 (2016).
- Martin-Iguacel, R., Negrodo, E., Peck, R. & Friis-Moller, N. Hypertension Is a Key Feature of the Metabolic Syndrome in Subjects Aging with HIV. *Curr Hypertens Rep* **18**, 46, doi: 10.1007/s11906-016-0656-3 (2016).
- Nasi, M. *et al.* Aging and inflammation in patients with HIV infection. *Clin Exp Immunol*, doi: 10.1111/cei.12814 (2016).
- Nduka, C., Sarki, A., Uthman, O. & Stranges, S. Impact of antiretroviral therapy on serum lipoprotein levels and dyslipidemias: a systematic review and meta-analysis. *Int J Cardiol* **199**, 307–318, doi: 10.1016/j.ijcard.2015.07.052 (2015).
- d'Ettoire, G. *et al.* What happens to cardiovascular system behind the undetectable level of HIV viremia? *AIDS Res Ther* **13**, 21, doi: 10.1186/s12981-016-0105-z (2016).
- Haas, D. W. & Tarr, P. E. Perspectives on pharmacogenomics of antiretroviral medications and HIV-associated comorbidities. *Curr Opin HIV AIDS* **10**, 116–122, doi: 10.1097/COH.0000000000000134 (2015).
- Manji, H., Jager, H. R. & Winston, A. HIV, dementia and antiretroviral drugs: 30 years of an epidemic. *J Neurol Neurosurg Psychiatry* **84**, 1126–1137, doi: 10.1136/jnnp-2012-304022 (2013).
- Chen, H. *et al.* Peripheral neuropathy in ART-experienced patients: prevalence and risk factors. *J Neurovirol* **19**, 557–564, doi: 10.1007/s13365-013-0216-4 (2013).
- Neuman, M. G., Schneider, M., Nanau, R. M. & Parry, C. HIV-Antiretroviral Therapy Induced Liver, Gastrointestinal, and Pancreatic Injury. *Int J Hepatol* **2012**, 760706, doi: 10.1155/2012/760706 (2012).
- Oliveira, N. M., Ferreira, F. A., Yonamine, R. Y. & Cheher, E. Z. Antiretroviral drugs and acute pancreatitis in HIV/AIDS patients: is there any association? A literature review. *Einstein (Sao Paulo)* **12**, 112–119 (2014).
- Dikman, A. E., Schonfeld, E., Srisarajivakul, N. C. & Poles, M. A. Human Immunodeficiency Virus-Associated Diarrhea: Still an Issue in the Era of Antiretroviral Therapy. *Dig Dis Sci* **60**, 2236–2245, doi: 10.1007/s10620-015-3615-y (2015).
- Estrada, V. *et al.* Relationship between plasma bilirubin level and oxidative stress markers in HIV-infected patients on atazanavir- vs. efavirenz-based antiretroviral therapy. *HIV Med*, doi: 10.1111/hiv.12368 (2016).
- Laprise, C., Baril, J. G., Dufresne, S. & Trottier, H. Atazanavir and other determinants of hyperbilirubinemia in a cohort of 1150 HIV-positive patients: results from 9 years of follow-up. *AIDS Patient Care STDS* **27**, 378–386, doi: 10.1089/apc.2013.0009 (2013).
- Guaraldi, G., Stentarelli, C., Zona, S. & Santoro, A. HIV-associated lipodystrophy: impact of antiretroviral therapy. *Drugs* **73**, 1431–1450, doi: 10.1007/s40265-013-0108-1 (2013).
- Margolis, A. M., Heverling, H., Pham, P. A. & Stolbach, A. A review of the toxicity of HIV medications. *J Med Toxicol* **10**, 26–39, doi: 10.1007/s13181-013-0325-8 (2014).
- Dragovic, G. & Jevtovic, D. The role of nucleoside reverse transcriptase inhibitors usage in the incidence of hyperlactatemia and lactic acidosis in HIV/AIDS patients. *Biomed Pharmacother* **66**, 308–311, doi: 10.1016/j.biopha.2011.09.016 (2012).
- Wu, X., Li, Y., Peng, K. & Zhou, H. HIV protease inhibitors in gut barrier dysfunction and liver injury. *Curr Opin Pharmacol* **19**, 61–66, doi: 10.1016/j.coph.2014.07.008 (2014).
- Diaz-Delfin, J. *et al.* Effects of nevirapine and efavirenz on human adipocyte differentiation, gene expression, and release of adipokines and cytokines. *Antiviral Res* **91**, 112–119, doi: 10.1016/j.antiviral.2011.04.018 (2011).
- Calmy, A., Hirschel, B., Cooper, D. A. & Carr, A. A new era of antiretroviral drug toxicity. *Antivir Ther* **14**, 165–179 (2009).
- Apostolova, N. *et al.* Involvement of nitric oxide in the mitochondrial action of efavirenz: a differential effect on neurons and glial cells. *J Infect Dis* **211**, 1953–1958, doi: 10.1093/infdis/jiu825 (2015).
- Purnell, P. R. & Fox, H. S. Efavirenz induces neuronal autophagy and mitochondrial alterations. *J Pharmacol Exp Ther* **351**, 250–258, doi: 10.1124/jpet.114.217869 (2014).
- Apostolova, N. *et al.* ER stress in human hepatic cells treated with Efavirenz: mitochondria again. *J Hepatol* **59**, 780–789, doi: 10.1016/j.jhep.2013.06.005 (2013).
- Bertrand, L. & Toborek, M. Dysregulation of Endoplasmic Reticulum Stress and Autophagic Responses by the Antiretroviral Drug Efavirenz. *Mol Pharmacol* **88**, 304–315, doi: 10.1124/mol.115.098590 (2015).
- Chow, F. C. HIV infection, vascular disease, and stroke. *Semin Neurol* **34**, 35–46, doi: 10.1055/s-0034-1372341 (2014).
- Quiros-Roldan, E. *et al.* Incidence of cardiovascular events in HIV-positive patients compared to general population over the last decade: a population-based study from 2000 to 2012. *AIDS Care*, 1–8, doi: 10.1080/09540121.2016.1198750 (2016).
- Ovbiagele, B. & Nath, A. Increasing incidence of ischemic stroke in patients with HIV infection. *Neurology* **76**, 444–450, doi: 10.1212/WNL.0b013e31820a0cfc (2011).
- Dobbs, M. R. & Berger, J. R. Stroke in HIV infection and AIDS. *Expert Rev Cardiovasc Ther* **7**, 1263–1271, doi: 10.1586/erc.09.72 (2009).
- Benjamin, L. A. *et al.* HIV infection and stroke: current perspectives and future directions. *Lancet Neurol* **11**, 878–890, doi: 10.1016/S1474-4422(12)70205-3 (2012).
- Chow, F. C. *et al.* Comparison of ischemic stroke incidence in HIV-infected and non-HIV-infected patients in a US health care system. *J Acquir Immune Defic Syndr* **60**, 351–358, doi: 10.1097/QAI.0b013e31825c7f24 (2012).

32. Hanna, D. B. *et al.* HIV Infection Is Associated With Progression of Subclinical Carotid Atherosclerosis. *Clin Infect Dis* **61**, 640–650, doi: 10.1093/cid/civ325 (2015).
33. Cruse, B., Cysique, L. A., Markus, R. & Brew, B. J. Cerebrovascular disease in HIV-infected individuals in the era of highly active antiretroviral therapy. *J Neurovirol* **18**, 264–276, doi: 10.1007/s13365-012-0092-3 (2012).
34. Gomez-Garre, D. *et al.* Association of HIV-Infection and antiretroviral therapy with levels of endothelial progenitor cells and subclinical atherosclerosis. *J Acquir Immune Defic Syndr* **61**, 545–551, doi: 10.1097/QAI.0b013e31826afbfc (2012).
35. Grinspoon, S. & Carr, A. Cardiovascular risk and body-fat abnormalities in HIV-infected adults. *N Engl J Med* **352**, 48–62, doi: 10.1056/NEJMra041811 (2005).
36. Weiss, M. *et al.* Efavirenz Causes Oxidative Stress, Endoplasmic Reticulum Stress, and Autophagy in Endothelial Cells. *Cardiovasc Toxicol* **16**, 90–99, doi: 10.1007/s12012-015-9314-2 (2016).
37. Borsari, M. *et al.* HIV infection and antiretroviral therapy lead to unfolded protein response activation. *Virol J* **12**, 77, doi: 10.1186/s12985-015-0298-0 (2015).
38. Hattab, S. *et al.* Soluble biomarkers of immune activation and inflammation in HIV infection: impact of 2 years of effective first-line combination antiretroviral therapy. *HIV Med* **16**, 553–562, doi: 10.1111/hiv.12257 (2015).
39. Moren, C. *et al.* Mitochondrial and apoptotic *in vitro* modelling of differential HIV-1 progression and antiretroviral toxicity. *J Antimicrob Chemother* **70**, 2330–2336, doi: 10.1093/jac/dkv101 (2015).
40. Keane, J. & Campbell, M. The dynamic blood-brain barrier. *FEBS J* **282**, 4067–4079, doi: 10.1111/febs.13412 (2015).
41. Qosa, H., Miller, D. S., Pasinelli, P. & Trotti, D. Regulation of ABC efflux transporters at blood-brain barrier in health and neurological disorders. *Brain Res* **1628**, 298–316, doi: 10.1016/j.brainres.2015.07.005 (2015).
42. Hawkins, R. A., O’Kane, R. L., Simpson, I. A. & Vina, J. R. Structure of the blood-brain barrier and its role in the transport of amino acids. *J Nutr* **136**, 218S–226S (2006).
43. Cornford, E. M. & Hyman, S. Localization of brain endothelial luminal and abluminal transporters with immunogold electron microscopy. *NeuroRx* **2**, 27–43, doi: 10.1602/neuroRx.2.1.27 (2005).
44. Daneman, R. & Prat, A. The blood-brain barrier. *Cold Spring Harb Perspect Biol* **7**, a020412, doi: 10.1101/cshperspect.a020412 (2015).
45. Filosa, J. A., Morrison, H. W., Iddings, J. A., Du, W. & Kim, K. J. Beyond neurovascular coupling, role of astrocytes in the regulation of vascular tone. *Neuroscience* **323**, 96–109, doi: 10.1016/j.neuroscience.2015.03.064 (2016).
46. Sweeney, M. D., Ayyadurai, S. & Zlokovic, B. V. Pericytes of the neurovascular unit: key functions and signaling pathways. *Nat Neurosci* **19**, 771–783, doi: 10.1038/nn.4288 (2016).
47. Obermeier, B., Daneman, R. & Ransohoff, R. M. Development, maintenance and disruption of the blood-brain barrier. *Nat Med* **19**, 1584–1596, doi: 10.1038/nm.3407 (2013).
48. Frechou, M. *et al.* Intranasal delivery of progesterone after transient ischemic stroke decreases mortality and provides neuroprotection. *Neuropharmacology* **97**, 394–403, doi: 10.1016/j.neuropharm.2015.06.002 (2015).
49. Yang, Y. *et al.* Attenuation of acute stroke injury in rat brain by minocycline promotes blood-brain barrier remodeling and alternative microglia/macrophage activation during recovery. *J Neuroinflammation* **12**, 26, doi: 10.1186/s12974-015-0245-4 (2015).
50. Pfefferkorn, T. & Rosenberg, G. A. Closure of the blood-brain barrier by matrix metalloproteinase inhibition reduces rtPA-mediated mortality in cerebral ischemia with delayed reperfusion. *Stroke* **34**, 2025–2030, doi: 10.1161/01.STR.0000083051.93319.28 (2003).
51. Adachi, T. *et al.* Endoplasmic reticulum stress induces retinal endothelial permeability of extracellular-superoxide dismutase. *Free Radic Res* **45**, 1083–1092, doi: 10.3109/10715762.2011.595408 (2011).
52. Fonseca, A. C., Ferreira, E., Oliveira, C. R., Cardoso, S. M. & Pereira, C. F. Activation of the endoplasmic reticulum stress response by the amyloid-beta 1–40 peptide in brain endothelial cells. *Biochim Biophys Acta* **1832**, 2191–2203, doi: 10.1016/j.bbdis.2013.08.007 (2013).
53. Ko, A. R., Kim, J. Y., Hyun, H. W. & Kim, J. E. Endothelial NOS activation induces the blood-brain barrier disruption via ER stress following status epilepticus. *Brain Res* **1622**, 163–173, doi: 10.1016/j.brainres.2015.06.020 (2015).
54. Maingat, F. *et al.* Inflammation and epithelial cell injury in AIDS enteropathy: involvement of endoplasmic reticulum stress. *FASEB J* **25**, 2211–2220, doi: 10.1096/fj.10-175992 (2011).
55. Murugan, D., Lau, Y. S., Lau, C. W., Mustafa, M. R. & Huang, Y. Angiotensin 1–7 Protects against Angiotensin II-Induced Endoplasmic Reticulum Stress and Endothelial Dysfunction via Mas Receptor. *PLoS One* **10**, e0145413, doi: 10.1371/journal.pone.0145413 (2015).
56. Tampakakis, E. *et al.* Intravenous Lipid Infusion Induces Endoplasmic Reticulum Stress in Endothelial Cells and Blood Mononuclear Cells of Healthy Adults. *J Am Heart Assoc* **5**, doi: 10.1161/JAHA.115.002574 (2016).
57. Persidsky, Y. *et al.* Rho-mediated regulation of tight junctions during monocyte migration across the blood-brain barrier in HIV-1 encephalitis (HIVE). *Blood* **107**, 4770–4780, doi: 10.1182/blood-2005-11-4721 (2006).
58. Leda, A. R., Dygert, L., Bertrand, L. & Toborek, M. Mouse Microsurgery Infusion Technique for Targeted Substance Delivery into the CNS via the Internal Carotid Artery. *JOVE* (2016).
59. Bertrand, L., Dygert, L. & Toborek, M. Induction of ischemic stroke and ischemia-reperfusion in mice using the middle artery occlusion technique and visualization of infarct area. *JOVE* (2016).
60. Martinez-Picado, J. & Deeks, S. G. Persistent HIV-1 replication during antiretroviral therapy. *Curr Opin HIV AIDS* **11**, 417–423, doi: 10.1097/COH.0000000000000287 (2016).
61. Liao, Z. *et al.* Specific binding of a mutated fragment of Clostridium perfringens enterotoxin to endothelial claudin-5 and its modulation of cerebral vascular permeability. *Neuroscience* **327**, 53–63, doi: 10.1016/j.neuroscience.2016.04.013 (2016).
62. Ku, J. M. *et al.* Protective actions of des-acylated ghrelin on brain injury and blood-brain barrier disruption after stroke in mice. *Clin Sci (Lond)*, doi: 10.1042/CS20160077 (2016).
63. Wang, Y. *et al.* Rhubarb attenuates blood-brain barrier disruption via increased zonula occludens-1 expression in a rat model of intracerebral hemorrhage. *Exp Ther Med* **12**, 250–256, doi: 10.3892/etm.2016.3330 (2016).
64. Xu, Z. M., Yuan, F., Liu, Y. L., Ding, J. & Tian, H. L. Glibenclamide attenuates blood-brain barrier disruption in adult mice following traumatic brain injury. *J Neurotrauma*, doi: 10.1089/neu.2016.4491 (2016).
65. Ren, C. *et al.* Limb Ischemic Preconditioning Attenuates Blood-Brain Barrier Disruption by Inhibiting Activity of MMP-9 and Occludin Degradation after Focal Cerebral Ischemia. *Aging Dis* **6**, 406–417, doi: 10.14336/AD.2015.0812 (2015).
66. Nitta, T. *et al.* Size-selective loosening of the blood-brain barrier in claudin-5-deficient mice. *J Cell Biol* **161**, 653–660, doi: 10.1083/jcb.200302070 (2003).
67. Cominacini, L. *et al.* Endoplasmic reticulum stress and Nrf2 signaling in cardiovascular diseases. *Free Radic Biol Med* **88**, 233–242, doi: 10.1016/j.freeradbiomed.2015.05.027 (2015).
68. Liu, T. *et al.* Coronary Microembolization Induces Cardiomyocyte Apoptosis Through the LOX-1-Dependent Endoplasmic Reticulum Stress Pathway Involving JNK/P38 MAPK. *Can J Cardiol* **31**, 1272–1281, doi: 10.1016/j.cjca.2015.01.013 (2015).
69. Roy, S., Trudeau, K., Roy, S., Tien, T. & Barrette, K. F. Mitochondrial dysfunction and endoplasmic reticulum stress in diabetic retinopathy: mechanistic insights into high glucose-induced retinal cell death. *Curr Clin Pharmacol* **8**, 278–284 (2013).
70. Matsumoto, T. *et al.* Diabetes and Age-Related Differences in Vascular Function of Renal Artery: Possible Involvement of Endoplasmic Reticulum Stress. *Rejuvenation Res* **19**, 41–52, doi: 10.1089/rej.2015.1662 (2016).
71. Cimellaro, A., Perticone, M., Fiorentino, T. V., Sciacqua, A. & Hribal, M. L. Role of endoplasmic reticulum stress in endothelial dysfunction. *Nutr Metab Cardiovasc Dis*, doi: 10.1016/j.numecd.2016.05.008 (2016).

72. Adachi, T., Teramachi, M., Yasuda, H., Kamiya, T. & Hara, H. Contribution of p38 MAPK, NF-kappaB and glucocorticoid signaling pathways to ER stress-induced increase in retinal endothelial permeability. *Arch Biochem Biophys* **520**, 30–35, doi: 10.1016/j.abb.2012.01.014 (2012).
73. Shin, J. A., Yoon, J. C., Kim, M. & Park, E. M. Activation of classical estrogen receptor subtypes reduces tight junction disruption of brain endothelial cells under ischemia/reperfusion injury. *Free Radic Biol Med* **92**, 78–89, doi: 10.1016/j.freeradbiomed.2016.01.010 (2016).
74. Liang, X. *et al.* Advanced oxidation protein products induce endothelial-to-mesenchymal transition in human renal glomerular endothelial cells through induction of endoplasmic reticulum stress. *J Diabetes Complications* **30**, 573–579, doi: 10.1016/j.jdiacomp.2016.01.009 (2016).
75. Awan, F. M. *et al.* In-silico analysis of claudin-5 reveals novel putative sites for post-translational modifications: Insights into potential molecular determinants of blood-brain barrier breach during HIV-1 infiltration. *Infect Genet Evol* **27**, 355–365, doi: 10.1016/j.meegid.2014.07.022 (2014).
76. Yamamoto, M. *et al.* Phosphorylation of claudin-5 and occludin by rho kinase in brain endothelial cells. *Am J Pathol* **172**, 521–533, doi: 10.2353/ajpath.2008.070076 (2008).
77. Sakurada, S. *et al.* Ca²⁺-dependent activation of Rho and Rho kinase in membrane depolarization-induced and receptor stimulation-induced vascular smooth muscle contraction. *Circ Res* **93**, 548–556, doi: 10.1161/01.RES.0000090998.08629.60 (2003).
78. Potash, M. J. *et al.* A mouse model for study of systemic HIV-1 infection, antiviral immune responses, and neuroinvasiveness. *Proc Natl Acad Sci USA* **102**, 3760–3765, doi: 10.1073/pnas.0500649102 (2005).
79. Hadas, E. *et al.* Transmission of chimeric HIV by mating in conventional mice: prevention by pre-exposure antiretroviral therapy and reduced susceptibility during estrus. *Dis Model Mech* **6**, 1292–1298, doi: 10.1242/dmm.012617 (2013).
80. He, H. *et al.* Enhanced human immunodeficiency virus Type 1 expression and neuropathogenesis in knockout mice lacking Type I interferon responses. *J Neuropathol Exp Neurol* **73**, 59–71, doi: 10.1097/NEN.0000000000000026 (2014).
81. Sindberg, G. M. *et al.* An infectious murine model for studying the systemic effects of opioids on early HIV pathogenesis in the gut. *J Neuroimmune Pharmacol* **10**, 74–87, doi: 10.1007/s11481-014-9574-9 (2015).
82. Ferguson, D., Clarke, S., Berry, N. & Almond, N. Attenuated SIV causes persisting neuroinflammation in the absence of a chronic viral load and neurotoxic ART. *AIDS*, doi: 10.1097/QAD.0000000000001178 (2016).
83. Tan, S. *et al.* HIV-1 impairs human retinal pigment epithelial barrier function: possible association with the pathogenesis of HIV-associated retinopathy. *Lab Invest* **94**, 777–787, doi: 10.1038/labinvest.2014.72 (2014).
84. Huang, W., Eum, S. Y., Andras, I. E., Hennig, B. & Toborek, M. PPARalpha and PPARgamma attenuate HIV-induced dysregulation of tight junction proteins by modulations of matrix metalloproteinase and proteasome activities. *FASEB J* **23**, 1596–1606, doi: 10.1096/fj.08-121624 (2009).
85. Zhong, Y., Zhang, B., Eum, S. Y. & Toborek, M. HIV-1 Tat triggers nuclear localization of ZO-1 via Rho signaling and cAMP response element-binding protein activation. *J Neurosci* **32**, 143–150, doi: 10.1523/JNEUROSCI.4266-11.2012 (2012).
86. Smith, C. J. *et al.* Trends in underlying causes of death in people with HIV from 1999 to 2011 (D:A:D): a multicohort collaboration. *Lancet* **384**, 241–248, doi: 10.1016/S0140-6736(14)60604-8 (2014).
87. Aldaz, P. *et al.* Mortality by causes in HIV-infected adults: comparison with the general population. *BMC Public Health* **11**, 300, doi: 10.1186/1471-2458-11-300 (2011).
88. Cima, M. *et al.* Cause of death in HIV-infected patients in South Carolina (2005–2013). *Int J STD AIDS* **27**, 25–32, doi: 10.1177/0956462415571970 (2016).
89. Weksler, B., Romero, I. A. & Couraud, P. O. The hCMEC/D3 cell line as a model of the human blood brain barrier. *Fluids Barriers CNS* **10**, 16, doi: 10.1186/2045-8118-10-16 (2013).
90. Usach, I., Melis, V. & Peris, J. E. Non-nucleoside reverse transcriptase inhibitors: a review on pharmacokinetics, pharmacodynamics, safety and tolerability. *J Int AIDS Soc* **16**, 1–14, doi: 10.7448/IAS.16.1.18567 (2013).
91. Marzolini, C. *et al.* Efavirenz plasma levels can predict treatment failure and central nervous system side effects in HIV-1-infected patients. *AIDS* **15**, 71–75 (2001).
92. Wolff, G., Davidson, S. J., Wrobel, J. K. & Toborek, M. Exercise maintains blood-brain barrier integrity during early stages of brain metastasis formation. *Biochem Biophys Res Commun* **463**, 811–817, doi: 10.1016/j.bbrc.2015.04.153 (2015).
93. Wrobel, J. K., Wolff, G., Xiao, R., Power, R. F. & Toborek, M. Dietary Selenium Supplementation Modulates Growth of Brain Metastatic Tumors and Changes the Expression of Adhesion Molecules in Brain Microvessels. *Biol Trace Elem Res* **172**, 395–407, doi: 10.1007/s12011-015-0595-x (2016).
94. Zhang, B. *et al.* Deficiency of telomerase activity aggravates the blood-brain barrier disruption and neuroinflammatory responses in a model of experimental stroke. *J Neurosci Res* **88**, 2859–2868, doi: 10.1002/jnr.22450 (2010).
95. Park, M., Kim, H. J., Lim, B., Wylegala, A. & Toborek, M. Methamphetamine-induced occludin endocytosis is mediated by the Arp2/3 complex-regulated actin rearrangement. *J Biol Chem* **288**, 33324–33334, doi: 10.1074/jbc.M113.483487 (2013).
96. Bagasra, O. Protocols for the *in situ* PCR-amplification and detection of mRNA and DNA sequences. *Nat Protoc* **2**, 2782–2795, doi: 10.1038/nprot.2007.395 (2007).

Acknowledgements

ARVds were obtained from the NIH AIDS Reagent Program, Pathogenesis and Basic Research Branch, Division of AIDS NIAID. EcoHIV-NDK viral plasmid was obtained from Dr. David J. Volsky, Icahn School of Medicine at Mt. Sinai, New York, NY. This work was supported by the NIH (MH098891, MH072567, HL126559, DA039576, DA027569), and by the Miami Center for AIDS Research funded by NIH Grant MH063022). LB is supported by an AHA postdoctoral fellowship (16POST31170002).

Author Contributions

L.B. and M.T. participated in research design, wrote or contributed to the writing of the manuscript, and provided funding; L.B. and L.D. conducted experiments; L.B. performed data analysis.

Additional Information

Supplementary information accompanies this paper at <http://www.nature.com/srep>

Competing financial interests: The authors declare no competing financial interests.

How to cite this article: Bertrand, L. *et al.* Antiretroviral Treatment with Efavirenz Disrupts the Blood-Brain Barrier Integrity and Increases Stroke Severity. *Sci. Rep.* **6**, 39738; doi: 10.1038/srep39738 (2016).

Publisher's note: Springer Nature remains neutral with regard to jurisdictional claims in published maps and institutional affiliations.



This work is licensed under a Creative Commons Attribution 4.0 International License. The images or other third party material in this article are included in the article's Creative Commons license, unless indicated otherwise in the credit line; if the material is not included under the Creative Commons license, users will need to obtain permission from the license holder to reproduce the material. To view a copy of this license, visit <http://creativecommons.org/licenses/by/4.0/>

© The Author(s) 2016